

# Pathways to double ionization of atoms in strong fields

Krzysztof Sacha<sup>1,2</sup> and Bruno Eckhardt<sup>1</sup>

<sup>1</sup> *Fachbereich Physik, Philipps Universität Marburg, D-35032 Marburg, Germany*

<sup>2</sup> *Instytut Fizyki im. Mariana Smoluchowskiego, Uniwersytet Jagielloński, ul. Reymonta 4, PL-30-059 Kraków, Poland*  
(November 20, 2018)

We discuss the final stages of double ionization of atoms in a strong linearly polarized laser field within a classical model. We propose that all trajectories leading to non-sequential double ionization pass close to a saddle in phase space which we identify and characterize. The saddle lies in a two degree of freedom subspace of symmetrically escaping electrons. The distribution of longitudinal momenta of ions as calculated within the subspace shows the double hump structure observed in experiments. Including a symmetric bending mode of the electrons allows us to reproduce the transverse ion momenta. We discuss also a path to sequential ionization and show that it does not lead to the observed momentum distributions.

32.80.Fb, 32.80.Rm, 05.45.Mt

## I. INTRODUCTION

Present day lasers are powerful enough to ionize several electrons from an atom. The electrons can be removed one by one in a sequential process or all at once in a non-sequential process. Independent electron models give ionization rates that are much smaller than experimentally observed [1], indicating that interactions between electrons are important. A series of most recent experiments has added the observation that also the final state of the electrons is dominated by the interactions: the total momentum of the electrons is aligned along the field axis [2–5] and the joint distribution of parallel momenta for the two electrons, in the double ionization experiment [5], has pronounced maxima along the diagonal, showing that the electrons typically come with the same momenta. These observations have been reproduced in numerical simulations with varying approximations and simplifying assumptions [6,7]. But given the complexity of the analysis that is required the essential elements are difficult to identify. As a step towards a better understanding we discuss here the pathways to double ionization within a classical model for electrons in a combined Coulomb and external field.

Our aim is not to describe the full ionization process all the way from the ground state to the final, multiply ionized state. According to the currently accepted models [8–13,6,7], the whole process of multiphoton multiple ionization can naturally be divided into two steps: in the first step a compound state of highly excited electrons close to the nucleus is formed and in the second step several electrons can escape from this compound state to produce the multiply ionized final state. We focus on the last step, the escape of two or more electrons from the highly excited compound state close to the nucleus.

The formation of the intermediate compound state is suggested by the rescattering model [8,9] for strong field multiple ionization. According to this model the enhanced cross section for multiple ionization is due to a rescattering of one electron that is temporarily ionized

and accelerated by the field before it returns to the nucleus when the field reverses. During the collision energy is transferred to other electrons, but all of this happens close to the core, where the dynamics of the electrons is fast and the interactions are strong and non-integrable. As a consequence, details of the initial preparation process are lost. Moreover, the decay of this state is also quick. The compound state is thus a short lived, highly unstable complex that separates the first half of the excitation process, whose main contribution is the build up of energy in the complex, from the second half, where the decay mode is determined.

The compound state has several decay paths: single ionization when only one electron escapes to infinity, double or multiple ionization with two or more electrons escaping to infinity, and the case of a single electron that escapes from the neighborhood of the nucleus but is rescattered to the next field reversal: in the latter case the whole process repeats itself, another compound state is formed and the decay path has to be selected anew.

We discuss here the further evolution after the formation of the compound state. To be specific, we will focus on the escape of two electrons in the following, but the arguments can easily be extended to the removal of more than two electrons. The main aim is to identify the channels that lead to double escape and to study their signatures in the distribution of electron and ion momenta. Our analysis is purely classical. Given the highly excited complex from which we start and the multiphoton nature of the process this seems a reasonable point of entry to the final stage of the ionization process. Our analysis is very similar to Wanniers approach [14–17] to double ionization by electron impact. There main difference is that in the present case one has to take into account also the external field. Brief summaries of some aspects of this model have been presented in [18,19].

The pathways to double ionization are discussed in section 2. The dynamics in the  $C_{2v}$  and  $C_v$  subspaces including the effective potential and sample trajectories is discussed in section 3. A key element of our argument is

the identification of a saddle in phase space near which trajectories leading to non-sequential double ionization have to pass; its properties and stability are discussed in section 4. The distributions of electron momenta within the  $C_{2v}$  and  $C_v$  subspaces are analyzed in section 5. The dynamics outside these symmetry spaces and sequential ionization processes are discussed in section 6. We conclude with a summary of the model in section 7.

## II. PATHWAYS TO DOUBLE IONIZATION

As described in the introduction we assume an initial state of two highly excited electrons near the nucleus which then decays to either single ionization or double ionization. During this process the linearly polarized laser field is always on. Therefore, the Hamiltonian consists of three parts,

$$H = T + V_i + V_{12} \quad (1)$$

the kinetic energy of the electrons,

$$T = \frac{\mathbf{p}_1^2}{2} + \frac{\mathbf{p}_2^2}{2} \quad (2)$$

the potential energies associated with the interaction with the nucleus and the field (polarized along  $z$ -axis),

$$V_i = -\frac{2}{|\mathbf{r}_1|} - \frac{2}{|\mathbf{r}_2|} + F(t)z_1 + F(t)z_2 \quad (3)$$

and the repulsion between the electrons,

$$V_{12} = \frac{1}{|\mathbf{r}_2 - \mathbf{r}_1|}. \quad (4)$$

The electric field strength  $F(t)$  has an oscillatory component times the envelope from the pulse; the discussion applies to general  $F(t)$ , and specific choices have to be made for the numerical simulations only.

Once the electrons leave the atom the repulsion pushes them apart and becomes weaker the larger the separation. Thus in the asymptotic state after ionization and after the pulse is turned off, repulsion is minimized. In order to identify the effects of the electron repulsion on the full process it is instructive to consider the double ionization events without repulsion first. This will be presented in the next section. The pathways with electron repulsion included will be presented thereafter.

### A. Without electron repulsion

The Hamiltonian for two electrons without electron repulsion splits into two independent Hamiltonians for each electron. In view of the fast motion of the electrons close to the nucleus we will frequently use an adiabatic assumption and discuss motion of the electrons in a field

with fixed amplitude  $F$ . Note, however, that all simulations use the full time-dependent field and do not make use of this adiabatic assumption. With this assumption each electron moves in a constant electric field, one of the few non-trivial integrable problems. The initial energy and the other constants of motion of each electron are fixed by the initial conditions (in the compound state) and do not change. Double ionization can thus occur only if both electrons individually have enough energy to ionize (and have the other constants of motion so as to allow ionization). The threshold for ionization is set by the field strength: if the field is non-zero a Stark saddle forms and the total energy has to be above the Stark saddle. For a constant field strength  $F$  the saddle lies at  $|z_F| = \sqrt{2/|F|}$  and has a potential energy (single electron)  $V_F = -2\sqrt{2|F|}$ . Therefore, double ionization is excluded if the total energy for both electrons is less than  $2V_F$ . For  $E = 2V_F$  the only path leading to double ionization has both electrons with the same energy. For  $E > 2V_F$  double ionization becomes possible even with slight asymmetries in the energy distribution.

In the full system of two electrons without repulsion but in a time-dependent field integrability is lost but separability is still preserved. As discussed in the introduction the initial state is a compound state with negative energy for each electron. If that energy is above the Stark saddle and if the motion is directed towards it the electrons can cross and run away from the nucleus. Once they cross the saddle they have to gain energy to escape from the Coulomb attraction when the field is turned off. This happens essentially by running down the potential energy slope on the other side of the saddle while the field is still on. This mechanism of energy gain is the same as in the interacting electron case.

### B. With electron repulsion

With the electron repulsion included the common Stark saddle at  $z_F$  is no longer accessible since the electrons cannot sit on top of each other. The best that can be achieved is a symmetric arrangement of both electrons in the same distance from the nucleus and symmetric with respect to the field axis. If the distances are not the same, electron repulsion will push the electron that is further out away from the nucleus and thus help towards ionization, but the one further in has to face not only Coulomb attraction but also the repulsion from the one further out. Thus repulsion acts so as to amplify differences in energy in this configuration. The configuration that is singled out is a symmetric one, with both electrons moving at the same distance from the nucleus. Deviations from this configuration will be amplified sufficiently so that non-sequential double ionization is suppressed and only single ionization takes place. A remaining electron can, however, be still ionized if its energy is higher than the saddle energy for a single electron

atom and, in the adiabatic picture, the other constants of motions allow to do so. In such sequential ionization correlations between escaping electrons are strongly weakened, that is the final momenta of the electrons along the polarization axis can be either parallel or anti-parallel.

### III. DYNAMICS IN THE $C_{2v}$ AND $C_v$ SUBSPACES

A two electron atom illuminated by a linearly polarized electromagnetic wave possesses some symmetry subspaces. The simplest  $C_{2v}$  symmetric configuration corresponds to both electrons moving in a plane which contains the field polarization axis and with positions and momenta symmetric with respect to this axis. The electrons put in such a configuration never leave it because there is no force which can pull them out of the subspace. The symmetry subspace can be enlarged. That is, with additional bending motion of the electrons with respect to the field axis the symmetry subspace is  $C_v$ .

The symmetric configurations become more apparent in suitably chosen coordinates. We apply the canonical transformation

$$\begin{aligned} R &= (\rho_1 + \rho_2)/2, & p_R &= p_{\rho_1} + p_{\rho_2} \\ r &= (\rho_1 - \rho_2)/2, & p_r &= p_{\rho_1} - p_{\rho_2} \\ Z &= (z_1 + z_2)/2, & p_Z &= p_{z_1} + p_{z_2} \\ z &= (z_1 - z_2)/2, & p_z &= p_{z_1} - p_{z_2}, \\ \varphi &= \varphi_1 + \varphi_2, & L &= (p_{\varphi_1} + p_{\varphi_2})/2 \\ \phi &= \varphi_1 - \varphi_2, & p_\phi &= (p_{\varphi_1} - p_{\varphi_2})/2 \end{aligned} \quad (5)$$

where  $(\rho_i, z_i, \varphi_i)$  are cylindrical coordinates of the electrons, labeled  $i = 1$  and  $2$ . For double ionization in linearly polarized laser field the total angular momentum projection on the polarization axis is conserved. The experiments begin with atoms in the ground state, thus, for the field directed along the  $z$ -axis we may choose  $L = 0$ . Then the Hamiltonian of the system reads

$$\begin{aligned} H &= \frac{p_R^2 + p_r^2 + p_Z^2 + p_z^2}{4} + \frac{p_\phi^2}{2(R+r)^2} \\ &+ \frac{p_\phi^2}{2(R-r)^2} + V(R, r, Z, z, \phi, t) \end{aligned} \quad (6)$$

with the potential energy

$$\begin{aligned} V &= -\frac{2}{\sqrt{(R+r)^2 + (Z+z)^2}} - \frac{2}{\sqrt{(R-r)^2 + (Z-z)^2}} \\ &+ \frac{1}{\sqrt{2R^2 - 2(R^2 - r^2)\cos\phi + 2r^2 + 4z^2}} \\ &+ 2ZF(t), \end{aligned} \quad (7)$$

where the field is given by  $F(t) = Ff(t)\cos(\omega t + \theta)$  with  $F$ ,  $\omega$  and  $\theta$  the peak amplitude, frequency and initial phase of the field, respectively, and with

$$f(t) = \sin^2(\pi t/T_d) \quad (8)$$

the pulse envelope of duration  $T_d$ .

Setting  $r = 0$ ,  $p_r = 0$ ,  $z = 0$  and  $p_z = 0$  we define the  $C_v$  symmetry subspace. The Hamiltonian is then reduced to

$$H = \frac{p_R^2 + p_Z^2}{4} + \frac{p_\phi^2}{R^2} + V(R, Z, \phi) \quad (9)$$

where

$$V = -\frac{4}{\sqrt{R^2 + Z^2}} + \frac{1}{R\sqrt{2(1 - \cos\phi)}} + 2ZF(t). \quad (10)$$

The potential (7) is symmetric in  $r$  (for  $z = 0$ ) and in  $z$  (for  $r = 0$ ), so that the derivatives with respect to  $r$  and  $z$  vanish: once the electrons are in the symmetry subspace  $r = z = 0$  and  $p_r = p_z = 0$ , they cannot leave it.

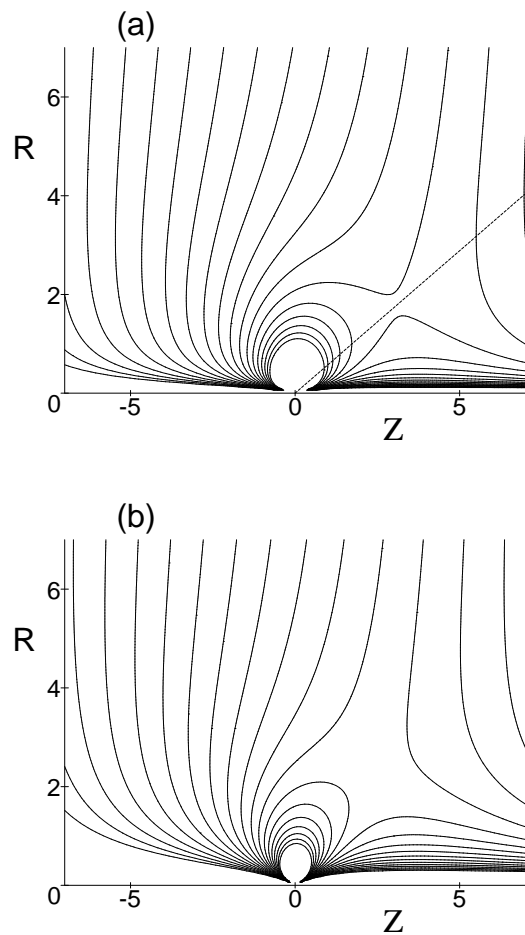


FIG. 1. Sections through equipotential surfaces of the adiabatic potential Eq. (10) for fixed time  $t$  and for  $\phi = \pi$  (a) and  $\phi = \pi/4$  (b). Panel (a) corresponds also to the potential Eq. (12) in the  $C_{2v}$  symmetric subspace; the saddle moves along the dashed line when the electric field points in the positive  $Z$ -direction and along a second obtained by reflection on  $Z = 0$  during the other half of the field cycle.

The further constraint  $\phi = \pi$  and  $p_\phi = 0$  leads to the  $C_{2v}$  symmetry subspace

$$H = \frac{p_R^2 + p_Z^2}{4} + V(R, Z) \quad (11)$$

with potential

$$V = -\frac{4}{\sqrt{R^2 + Z^2}} + \frac{1}{2R} + 2ZF(t). \quad (12)$$

Let us begin with an analysis of the motion in the  $C_{2v}$  subspace. The electrons move in a plane and their positions ( $\rho_i = R$ ,  $z_i = Z$ ) in that plane and their momenta ( $p_{\rho_i} = p_R/2$ ,  $p_{z_i} = p_Z/2$ ) are the same.

The adiabatic potential (12) for fixed time corresponding to the maximal field amplitude  $F = 0.137$  a.u., i.e. an intensity of  $6.6 \cdot 10^{14}$  W/cm<sup>2</sup>, is shown in Fig. 1a. The saddle is located along the line  $Z_S = r_S \cos \theta_S$  and  $R_S = r_S \sin \theta_S$  with  $\theta_S = \pi/6$  or  $5\pi/6$  and at a distance

$$r_S^2 = \sqrt{3}/|F(t)|. \quad (13)$$

The energy of the saddle is

$$V_S = -6\sqrt{|F(t)|/\sqrt{3}}. \quad (14)$$

For the above mentioned field the saddle has an energy of  $V_S = -1.69$  a.u..

If we switch off the repulsion between the electrons the saddle will move onto the  $Z$ -axis, i.e. both electrons are allowed to escape symmetrically on top of each other. With repulsion the saddle splits into two symmetrically related ones and moves away from the  $Z$ -axis.

A typical trajectory within the symmetric configuration for  $\omega = 0.057$  a.u. (800 nm) is shown in Fig. 2. During the ramping of the field the electronic motion is little influenced by the electric field, but during the third half cycle of the field the saddle is close enough to the electron orbits and ionization takes place. Once on the other side of the saddle, the electrons rapidly gain energy. The saddle thus provides a kind of transition state [20,21] for the correlated double ionization process: once the electrons cross it, they are accelerated by the field and pulled further away, making a return rather unlikely. Moreover, the electrons can acquire the missing energy so that both can escape to infinity even when the field vanishes. Note that before double ionization occurs the effect of the field on the electrons is minimal, supporting the adiabatic assumption.

In the experiments [2–5] ion momenta both parallel and transverse to the field are measured. For  $\omega = 0.057$  a.u. momentum transfer by photons is negligible, so the ion momentum reflects the sum of the momenta of the emitted electrons,  $\mathbf{p}_1 + \mathbf{p}_2 = -\mathbf{p}_{ion}$ . Symmetric motion in the  $C_{2v}$  subspace takes place in a plane and consequently the total transverse momentum of the electrons is zero. In the  $C_v$  subspace the electrons are

permitted to leave the plane, and this is a minimal extension necessary to give obtain non-vanishing transverse momenta.

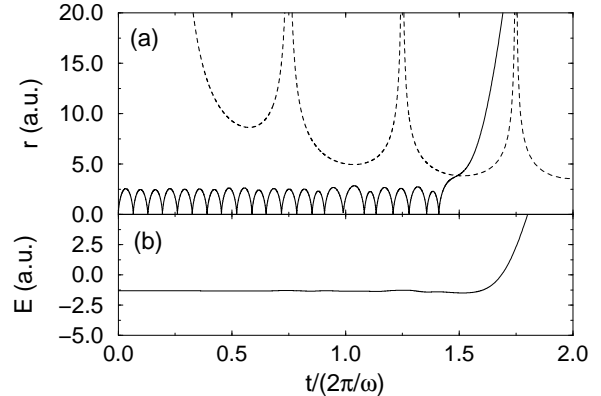


FIG. 2. A typical trajectory in the  $C_{2v}$  symmetric subspace with  $E = -1.3$  a.u.,  $F = 0.137$  a.u. and the pulse duration  $T_d = 4 \times 2\pi/\omega$ . Panel (a) distance of the electrons to the nucleus. The dashed line indicates the distance of the saddle. Note that before the double ionization occurs the effect of the field on the electrons is minimal, supporting the adiabatic assumption. Panel (b) energy of the electrons. Note that the initial state has negative total energy and cannot lead to double ionization. The energy increases once the electrons have escaped from the nucleus far enough so that acceleration by the electric field dominates.

The sections through equipotential surfaces of Eq. (10) for  $\phi = \pi$  and  $\phi = \pi/4$  are shown in Fig. 1. Increasing or decreasing  $\phi$  from  $\pi$  results in greater repulsion energy between the electrons. So the electrons can escape, with the coordinate  $\phi \neq \pi$ , only if the energy is greater than the saddle energy, Eq. (14).

We discuss here double ionization of atoms but the analysis of a symmetric escape can be easily extended to a multiple ionization process. Especially for  $N$  electrons the symmetric subspace corresponding to  $N$  particles symmetrically distributed in the plane perpendicular to the polarization axis is  $C_{Nv}$  [19].

#### IV. THE SADDLE

Within the adiabatic assumption and for a fixed external field strength non-sequential double ionization hinges on the crossing of the saddle in the  $C_{2v}$  subspace. For the dynamics within the subspace this is obvious from the potential. For the motion in the full six-dimensional configuration space this is less clear. One possibility to gain insight locally near the saddle is a harmonic analysis and a determination of the frequencies of small deviations. Within the  $C_{2v}$  symmetric subspace there is one hyperbolic mode corresponding to motion across the saddle (the ‘reaction coordinate’, in chemical physics parlance [20,21]) and a stable one corresponding to perpendicular

variations. In the full space we expect at least one additional unstable one, corresponding to the amplification of energy differences mentioned before in section (IIB). The analysis in this section is for fixed field strength, for electron dynamics in a constant external field, justified by the adiabatic reasoning.

The second order variations of the potential (7) around the saddle point results in

$$\begin{aligned}
H \approx & \frac{p_R^2 + p_Z^2}{4} + \frac{9}{2r_S^3}(R - R_S)^2 \\
& - \frac{3\sqrt{3}}{r_S^3}(R - R_S)(Z - Z_S) - \frac{5}{2r_S^3}(Z - Z_S)^2 \\
& + \frac{p_r^2 + p_z^2}{4} + \frac{1}{2r_S^3}r^2 - \frac{3\sqrt{3}}{r_S^3}rz - \frac{9}{2r_S^3}z^2 \\
& + \frac{p_\phi^2}{R_S^2} + \frac{1}{4R_S}(\phi - \pi)^2 + V_S.
\end{aligned} \tag{15}$$

The  $\phi$ -degree of freedom corresponds to a bending motion of the electrons against each other and is stable on account of the repulsive nature of the Coulomb force. This degree of freedom is also the one that comes in by going from the  $C_{2v}$  subspace to the  $C_v$  subspace.

Diagonalization in the  $(R - R_S, Z - Z_S)$  space reveals one stable and one unstable mode. The latter corresponds to the reaction coordinate and its Lyapunov exponent is  $\mu \approx 1.21F^{3/4}$ . Similar analysis in the  $(r, z)$  space yields another stable and unstable mode with Lyapunov exponent  $\nu \approx 1.57F^{3/4}$ . The direction of the unstable mode is  $(w_r, w_z) \approx (0.43w, w)$  and it corresponds to the situation when one electron escapes and the other one is turned back to the nucleus. That is, with positive and increasing  $w$  the first electron moves away from the nucleus, i.e.  $\rho_1 = R_S + w_r$  and  $z_1 = Z_S + w_z$  grow [see (5)], while the other one returns to the nucleus, i.e.  $\rho_1 = R_S - w_r$  and  $z_1 = Z_S - w_z$  decrease.

All in all there are three stable modes and two unstable ones. Any energy contained in the stable modes is preserved and cannot be transferred to kinetic energy along the reaction coordinates. Whether single or double ionization occurs is thus determined solely by the energy and initial conditions in the two hyperbolic subspaces. For energy equal to the saddle energy only a trajectory within the  $C_{2v}$  symmetry subspace leads to non-sequential escape – any deviation from the subspace are growing faster than the escape along the reaction coordinate since  $\nu > \mu$ . For energy higher than the saddle some deviations from the symmetry subspace are allowed. In particular, following Wanniers lead and Rosts generalization [14–17] it is possible to estimate the critical behavior for the double ionization cross section at threshold. It is algebraic with the exponent given by the ratio of the positive Lyapunov exponents of the unstable modes. A detailed discussion of this is outside the main line of our arguments here and will be given elsewhere.

It is instructive to actually calculate numbers for the Lyapunov exponents in the two directions. For lasers

with the maximal field strength of  $F = 0.137$  a.u. we find  $1/\mu = 3.7$  a.u. and  $1/\nu = 2.8$  a.u.. Compared to the period of the laser,  $2\pi/\omega = 110.2$  a.u. this is rather fast, indicating that the crossing of the saddle and the separation away from the double ionization manifold take place rather quickly. This justifies also our adiabatic analysis in this section.

## V. FINAL STATE MOMENTA DISTRIBUTION WITHIN THE SYMMETRIC SUBSPACES

So far we have discussed the phase space features in an adiabatic approximation for fixed field strengths. Now we will use this to draw conclusions about the experimentally observed signatures, specifically about the distributions of ion momenta in the final state. They can be calculated within the  $C_v$  subspace by averaging over all initial conditions and all phases of the field. That this is possible is connected with the instability of the saddle: all trajectories leading to the non-sequential ionization have to pass sufficiently close to the saddle and the symmetric subspace. It therefore is possible to estimate the behaviour near the subspace from the dynamics within the subspace.

### A. Parameters of the model

The rescattering of an electron leads to a highly excited complex of total energy  $E$  which is one of the parameters of our model. The maximal energy a rescattering electron can bring in has been estimated to be about  $3.17U_p$  [8,9], where  $U_p$  is the ponderomotive energy of an electron. For the weakest field used in the experiment on double ionization of He atoms [2] this maximal energy barely corresponds to the ionization energy of the  $\text{He}^{1+}$  ions. We therefore assume in the following that the highly excited complex has a negative initial energy,  $E < 0$ .

The absence of detailed knowledge of the structure of the initial compound nucleus suggests to average over the initial configurations. However, even for a negative energy and fixed time it is difficult to define a microcanonical distribution of initial conditions for the Hamiltonian (9) since, for non-zero external field, the system is open. Therefore, we choose for the calculations initial conditions from the energy shell that also lie in the hypersurface  $Z = 0$ . The results are not sensitive to a particular choice of the hypersurface but the one for  $Z = 0$  has the advantage that the dipole moment along the field is zero and the choice of the initial conditions does not depend on the initial field phase.

The second parameter, in addition to the energy, is the time  $t_0$  during the pulse Eq. (8) when the highly excited complex is formed. The rescattering event is not possible

at the beginning of the pulse, so one has to start simulations somewhere in the middle of the pulse. In Fig. 3 and 4 final distributions of ion momenta for the initial energy  $E = -0.1$  a.u., field strength  $F = 0.137$  a.u. and different initial time  $t_0$  are shown. The distributions of the transverse momenta are almost the same but the ones for the parallel momenta differ. The latter reveal a double hump structure with widths sensitive to the initial time.

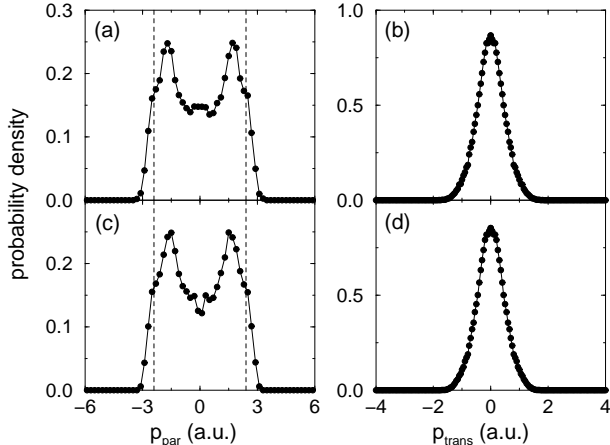


FIG. 3. Final distributions of ion momenta parallel,  $p_{par}$  and transverse,  $p_{trans}$  to the field polarization axis for the initial energy  $E = -0.1$  a.u., peak field amplitude  $F = 0.137$  a.u. and pulse duration  $T_d = 20 \times 2\pi/\omega$ . Panels (a)-(b) correspond to the initial time  $t_0 = 0.25T_d$  in the pulse duration with the envelop  $f(t) = \sin^2(\pi t/T_d)$  while panels (c)-(d) to  $t_0 = 0.75T_d$ . Dashed lines are related to the estimates  $\pm 2Ff(t_0)/\omega = \pm 2.4$  a.u.. Note that the distributions are essentially the same independently if one chooses  $t_0$  before or after the peak field value provided  $f(t_0)$  is the same. The results are based on integrations of about  $8 \cdot 10^4$  trajectories.

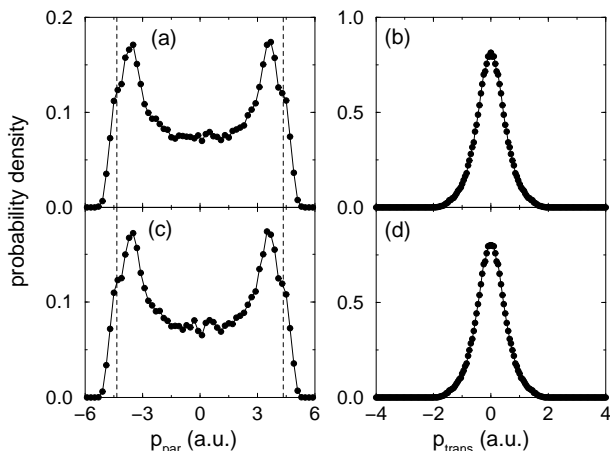


FIG. 4. The same as in Fig. 3 but for  $t_0 = 0.4T_d$  [panels (a)-(b)] and  $t_0 = 0.6T_d$  [panels (c)-(d)]. The width of the parallel momentum distribution can be estimated as  $\pm 2Ff(t_0)/\omega = \pm 4.3$  a.u..

The maximum energy that can be acquired by a free electron in the field is  $2U_p$ . So, for parallel emission of two electrons, the maximal parallel ion momentum can be estimated as

$$p_{par} = 2\sqrt{4U_p} = 2Ff(t)/\omega. \quad (16)$$

If we substitute in Eq. (16)  $t = t_0$  we find values which correspond very well to the widths of the distributions in Fig. 3 and 4. The figures indicate also that the widths are the same independently if  $t_0$  is chosen before or after the peak of the pulse provided  $f(t_0)$  is the same. This implies that the dominant ionizations take place in the first field cycle after the complex is formed. Fitting the width of the calculated distribution to the experimental results allows one to estimate the moment in the pulse when majority of doubly ionized ions are created.

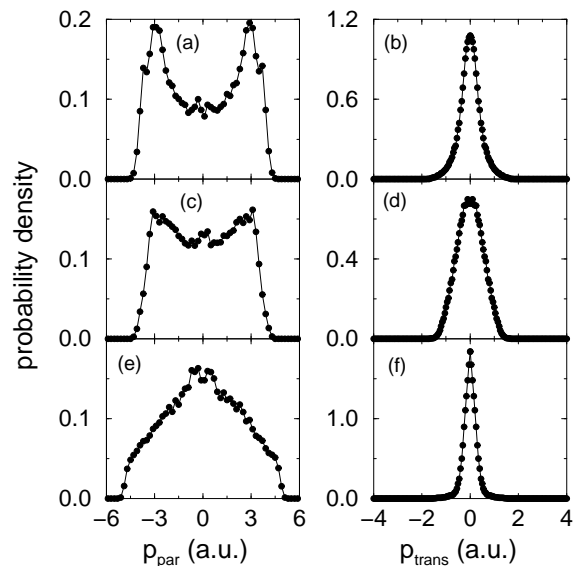


FIG. 5. The same as in Fig. 3-4 but for fixed  $t_0 = 0.33T_d$  and different initial energy:  $E = -0.05$  a.u. [panels (a)-(b)],  $E = -0.5$  a.u. [panels (c)-(d)] and  $E = -1.5$  a.u. [panels (e)-(f)].

Now we fix  $t_0$  and change the initial energy  $E$ ; the results are shown in Fig. 5. For the lowest energy,  $E = -1.5$  a.u., the transverse momentum distribution is narrower than for higher energies.  $E = -1.5$  a.u. is actually very close to the minimal saddle energy for the applied field,  $V_S = -1.69$  a.u.. Thus the effect is natural as, close to the saddle energy, only trajectories near the  $C_{2v}$  subspace can cross the saddle and those with  $\phi \neq \pi$  bounce back from the potential barrier and do not ionize.

While the width of the distributions of the parallel momenta do not change significantly their shapes do, especially for the initial energy close to the saddle. The electrons that cross the saddle when the energy is near  $V_S$  are slow and the combined interactions of the external and Coulomb fields shapes the distributions. This is different from the high energy case: then shortly after the

electrons cross the saddle the interaction with the electric field is stronger than the attraction to the nucleus and the distribution is mostly shaped by the laser field.

The initial energy of the complex is the higher the higher intensity of the laser is and the larger the energy a rescattered electron can bring in [8,9]. From the dependence of the distributions on the initial energy we may conclude that in the experiment the shape of the distribution of the parallel ion momenta should change character when the laser intensity increases. For the intensity at the threshold for non-sequential double ionization the distribution with single maximum around zero momentum is expected; for higher intensities the double hump structure should turn up.

All numerical results have been obtained for initial conditions taken from the  $C_v$  symmetry subspace. Our results for the  $C_{2v}$  subspace for parallel momentum distributions are essentially the same. The transverse momenta of ions for the  $C_{2v}$  subspace are, however, zero because of the symmetry assumption.

After this discussion of the two parameters (initial energy and starting time of the integration) we can turn to comparisons with experimental observations.

## B. Comparison with experimental results

Weber *et al.* [2] carried out double ionization experiments with He atoms and measured the distributions of ion momenta. They applied infrared (800 nm) laser pulses of the duration 220 fs (measured on the half peak value) and with the peak intensities in the range  $(2.9 - 6.6) \times 10^{14}$  W/cm<sup>2</sup>. In Fig. 6 and 7 we show the experimental distributions and compare with those calculated in the  $C_v$  subspace. The agreement is very good except for the parallel momentum distribution in Fig. 7 where the calculated distribution possesses a much more pronounced minimum than in the experiment and the positions of the peaks do not exactly coincide with the experimental values.

There are a few possible sources for these discrepancies. First, the pulse duration in the experiment was quite long, i.e. about 80 field cycles. The slow ramping of the field in the experiment implies that the initial time  $t_0$  of the ionization is less well defined, i.e. there are contributions from some range of  $t_0$ . There are also contributions from different initial energies. Secondly, real ionizing trajectories do not live exactly in the symmetry subspace but close to it, leading to asymmetries and additional differences in the final momenta. And there are also possible contributions from sequential double ionization events (see below).

Moshhammer *et al.* [4] performed experiments with Ne atoms for much shorter pulses, i.e. 30 fs and for radiation with similar wave length (795 nm) as the previous group. The comparison of our calculations with this experiment are presented in Fig. 8. Interactions of the two excited

electrons with the other electrons are neglected in our model and the energy values used in the calculations are measured with respect to the threshold for the two electron continuum (i.e. about 2.3 a.u.). The agreement is even better than for the case of He atoms. This is presumably due to the much shorter pulse duration and the fasted ramping of the field, so that the time  $t_0$  when the majority of the ionization events happen is much better defined.

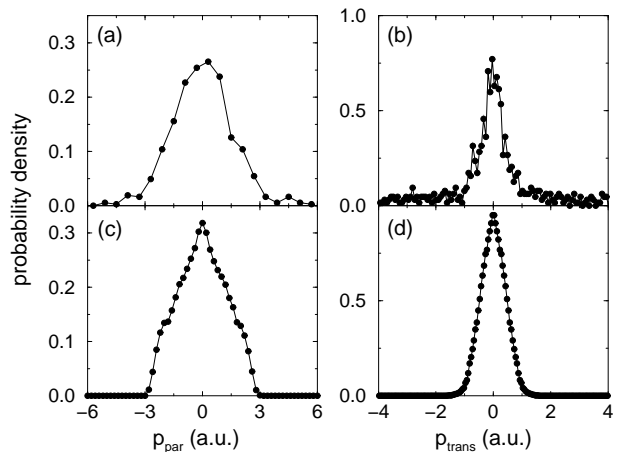


FIG. 6. Panels (a)-(b): final ion momentum distributions measured in the experiment of double ionization of He atoms in the focus of 800 nm, 220 fs (i.e. about  $80 \times 2\pi/\omega$ ) laser pulses at peak intensity of  $2.9 \times 10^{14}$  W/cm<sup>2</sup> (i.e. for the field strength  $F = 0.091$  a.u.) from [2]. Panels (c)-(d): the corresponding distributions calculated in the  $C_v$  symmetry subspace for the initial energy  $E = -0.6$  a.u. and  $t_0 = 0.33T_d$  where  $T_d/2 = 80 \times 2\pi/\omega$ , see Eq. 8.

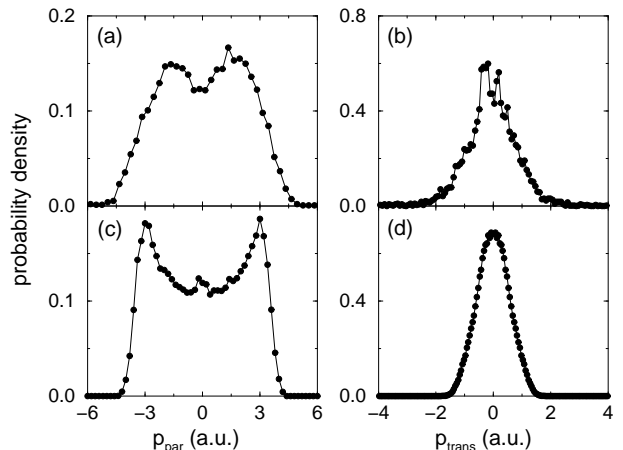


FIG. 7. Panels (a)-(b): the same as in the corresponding panels in Fig. 6 but for the peak intensity of  $6.6 \times 10^{14}$  W/cm<sup>2</sup> (i.e. for the field strength  $F = 0.137$  a.u.). Panels (c)-(d): the same as in the corresponding panels in Fig. 6 but for the initial energy  $E = -0.4$  a.u..

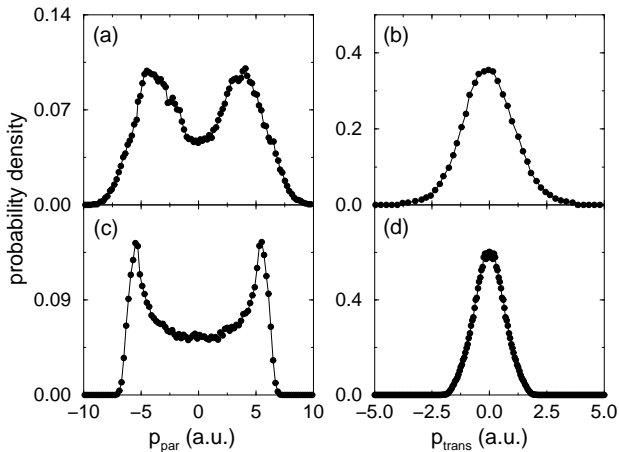


FIG. 8. Panels (a)-(b): final ion momentum distributions measured in the experiment of double ionization of Ne atoms in the focus of 795 nm, 30 fs (i.e. about  $11 \times 2\pi/\omega$ ) laser pulses at peak intensity of  $13 \times 10^{14}$  W/cm<sup>2</sup> (i.e. for the field strength  $F = 0.192$  a.u.) from [4]. Panels (c)-(d): the corresponding distributions calculated in the  $C_v$  symmetry subspace for the initial energy  $E = -0.3$  a.u. and  $t_0 = 0.4T_d$  where  $T_d/2 = 11 \times 2\pi/\omega$ , see Eq. 8.

## VI. SEQUENTIAL DOUBLE IONIZATION

Already from the experiment it is clear that double ionization is a rare process, e.g. outnumbered by single ionization by about  $10^4 : 1$  for He atoms and field intensity  $2.9 \cdot 10^{14}$  W/cm<sup>2</sup> [2]. Hence arbitrarily chosen initial conditions in the full space will typically not lead to double ionization and numerical simulations of the whole process are rather unattainable.

We have discussed the non-sequential double escape of the electrons considering trajectories within the symmetry subspace. Motion in the symmetry subspace is unstable, that is deviations from the subspace will be amplified leading to single rather than double ionization. We can illustrate this with trajectories started slightly outside the symmetry plane (Fig. 9). Fig 9a shows initial conditions on the saddle and symmetrically escaping electrons. For some deviation from symmetry, one electron escapes, the other remains trapped to the nucleus (Fig. 9b).

It is possible, however, that the second electron returns to the nucleus but picks up enough energy to ionize itself (Fig. 9c). In the adiabatic picture, if the energy of the remaining electron is higher than the saddle for a single electron atom,  $V_F = -2\sqrt{2|F|}$ , whether the electron stays trapped or escapes depends on the other constants of motion (besides the energy) in this integrable system. The second electron can thus escape during the same half field cycle as the first one but its final parallel momentum component need not be related to that of the first electron, as is shown in Fig. 9c.

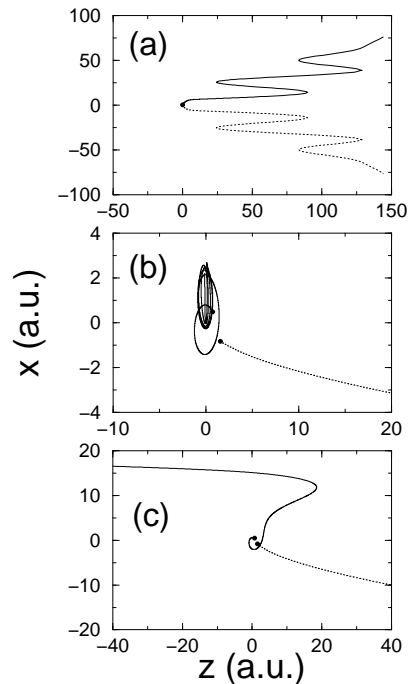


FIG. 9. Trajectories of electrons outside the symmetric subspace for  $E = -0.58$  a.u. and  $F = 0.137$  a.u.. Initial positions are close to the saddle and marked by heavy dots; the electrons are distinguished by dotted and continuous tracks. Panel (a) shows a symmetric escape of the electrons. Panel (b) shows a case where outside the symmetry subspace one electron escapes and the other falls back to the ion. Panel (c) shows an example of sequential ionization of both electrons in opposite directions.

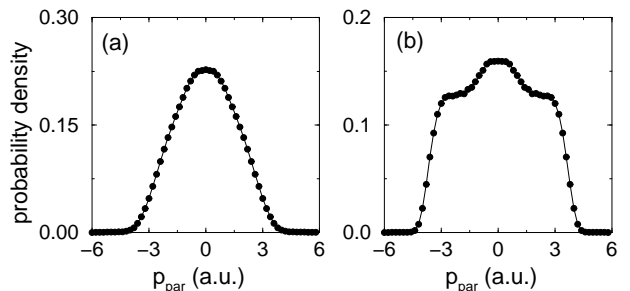


FIG. 10. Final parallel ion momenta distributions calculated in the two-dimensional non-interacting electrons model for the initial time  $t_0 = 0.33T_d$  in the pulse duration, where  $T_d = 20 \times 2\pi/\omega$ , peak field amplitude  $F = 0.137$  a.u. and initial energy  $E = -0.8$  a.u. [panel (a)] and  $E = -0.1$  a.u. [panel (b)]. The initial conditions for the electrons have been chosen to satisfy  $E = E_1 + E_2$  with the restrictions  $E_1 < 0$  and  $E_2 < 0$ . The saddle energy for a single electron is  $V_F = -1.05$  a.u.. The results in each panel are based on about  $1.5 \cdot 10^6$  trajectories.

We are not able to calculate the contribution of sequential events to the double ionization process but we can



estimate the distribution of the final ion momenta if the sequential process were dominant. To simulate sequential escape one may return to a non-interacting electron model, essentially since the electrons cross the barrier at different times. In the model the initial conditions for each electron are chosen independently, constrained only by the requirement that the total initial energy is fixed  $E = E_1 + E_2$  and that  $E_1 < 0$  and  $E_2 < 0$ . Simultaneous double ionization are not explicitly excluded, but events with delayed ionization are more probable, so that the distributions can still reflect the contributions from sequential ionization.

In Fig. 10 the distributions of parallel ion momenta for  $E = -0.8$  a.u. and  $E = -0.1$  a.u., calculated in the non-interacting electrons model for  $F = 0.137$  a.u. are plotted. The figure should be compared with the figures from the previous section. The conclusion is straightforward: the non-interacting electrons model is not able to reproduce correlations between the electrons observed in the experiments. Moreover, sequential escape can not be a dominant mechanism for double ionization in the range of the field intensities considered here.

## VII. CONCLUSIONS

We have considered the process of double ionization of atoms in a strong, linearly polarized field for intensities below the saturation of single electron ionization. We have developed a model for non-sequential double ionization within classical mechanics. The process has been divided into two stages: in the first one a rescattering process leads to a highly excited complex of two electrons. In the second stage, an ionization of such compound state takes place. We have focused on the latter stage considering different pathways to double escape of the electrons.

The excited complex can doubly ionize even when its energy is negative because the external field opens up saddles for electron escape. The pathway favored by the Coulomb interactions and the field is simultaneous symmetric escape of both electrons. Deviations from the symmetric configurations are amplified by the repulsion between the electrons which pulls one electron to infinity but the other one is pushed back to the nucleus. Therefore we propose that non-sequential double ionization is dominated by motions of electrons in or near the symmetric subspace with the saddle.

The requirement of the symmetric motion greatly simplifies the analysis which then can be carried out for the three- or even two-dimensional effective potential. The trajectory simulations within the symmetric configurations turns out to reproduce the experimentally observed ion momenta distributions very well. We have also considered an alternative mechanism of the ionization, i.e. sequential escape of the electrons. By means of the non-interacting electrons model we show that the sequential

ionization is not able to explain the experimentally observed electrons correlations.

The modeling of the experimental distributions requires information on two parameters, the initial energy and the time of formation, which reflect a lack of knowledge on the compound state and the ramping of the field. The dependence of the momentum distributions on the parameters and comparison with the experimental results give insights into the dynamics of double ionization.

The analysis in the present paper has been restricted to double ionization but its extension to multiple escape is straightforward [19]. In its current form the model is applicable for linearly polarized fields only. For other polarizations the number of rescattering events is greatly reduced. However, for some elliptically polarized field, if an electron is driven back to the core and a highly excited complex is formed, in the adiabatic approximation the symmetric configuration of the electrons can be defined with respect to the temporary electric field axis. Then one can proceed with the analysis as for the linearly polarized case.

Our whole discussion has a more than superficial similarity with Wanniers analysis of double ionization by electron impact [14–16]. The main differences are the presence of a field and its time dependence, which enlarges phase space and complicates the identification of the transition state. In the adiabatic approximation at fixed field strength we could identify this saddle in the  $C_{2v}$  subspace. The comparison with experiments is complicated furthermore by the necessity to average over initial energy and time of preparation of the compound state. Thus, signatures one might attribute to Wanniers analysis, such as threshold exponents (they follow immediately from the stability analysis of the saddle, but are not easy to verify), will be even more difficult to study. But we have no doubt that the observation of the correlated escape of the electrons [5] is a clear signature of the existence and dominance of the saddle and the pathways to double ionization which we discuss here.

## VIII. ACKNOWLEDGEMENTS

We would like to thank Harald Giessen for stimulating our interest in this problem and for discussions of the experiments. Financial support by the Alexander von Humboldt Foundation and by KBN under project 2P302B00915 are gratefully acknowledged.

- 
- [1] A. L’Huillier, L. A. Lompre, G. Mainfray, and C. Manus, *Phys. Rev. A* **27**, 2503 (1983).
  - [2] Th. Weber, M. Weckenbrock, A. Staudte, L. Spielberger, O. Jagutzki, V. Mergel, F. Afaneh, G. Urbasch, M.

- Vollmer, H. Giessen and R. Dörner, Phys. Rev. Lett. **84**, 443 (2000).
- [3] Th. Weber, M. Weckenbrock, A. Staudte, L. Spielberger, O. Jagutzki, V. Mergel, F. Afaneh, G. Urbasch, M. Vollmer, H. Giessen and R. Dörner, J. Phys. B: At. Mol. Opt. Phys. **33**, L1 (2000).
- [4] R. Moshhammer, B. Feuerstein, W. Schmitt, A. Dorn, C.D. Schöter, J. Ullrich, H. Rottke, C. Trump, M. Wittmann, G. Korn, K. Hoffmann and W. Sandner, Phys. Rev. Lett. **84**, 447 (2000).
- [5] Th. Weber, H. Giessen, M. Weckenbrock, G. Urbasch, A. Staudte, L. Spielberger, O. Jagutzki, V. Mergel, M. Vollmer, and R. Dörner, Nature **405**, 658 (2000).
- [6] A. Becker and F.H.M. Faisal, Phys. Rev. Lett. **84**, 3546 (2000).
- [7] R. Kopold, W. Becker, H. Rottke, and W. Sandner, (private communication).
- [8] P.B. Corkum, Phys. Rev. Lett. **71**, 1994 (1993).
- [9] K.C. Kulander, J. Cooper, and K.J. Schafer, Phys. Rev. A **51**, 561 (1995).
- [10] A. Becker and F.H.M. Faisal, J. Phys. B **29**, L197 (1996).
- [11] A. Becker and F.H.M. Faisal, J. Phys. B **32**, L335 (1999).
- [12] B. Sheehy, R. Lafon, M. Widmer, B. Walker, L.F. DiMauro, P.A. Agostini, and K.C. Kulander, Phys. Rev. A **58**, 3942 (1998).
- [13] A. Becker and F.H.M. Faisal, Phys. Rev. A **59**, R1742 (1999).
- [14] G.H. Wannier, Phys. Rev. **90**, 817 (1953).
- [15] A. R. P. Rau, Phys. Rep. **110**, 369, (1984).
- [16] J.M. Rost, Phys. Rep. **297**, 271 (1999).
- [17] J.M. Rost, (preprint).
- [18] B. Eckhardt and K. Sacha, physics/0005079; K. Sacha and B. Eckhardt, physics/0006013;
- [19] B. Eckhardt and K. Sacha, Physica Scripta (at press).
- [20] E. P. Wigner, Z. Phys. Chemie B **19**, 203 (1932); Trans. Faraday Soc. **3429**, (1938).
- [21] E. Pollak, in *Theory of Chemical Reactions*, vol III, M. Baer, ed., (CRC Press, Boca Raton, 1985, p. 123.